



Acetaminophen-induced Mitochondrial Oxidative Stress in Murine J774.2 Monocyte Macrophages

Thekra al-Belooshi, Annie John, Amna Al-Otaiba and Haider Raza*

Department of Biochemistry, Faculty of Medicine and Health Sciences, UAE University, POBox 17666, Al Ain, United Arab Emirates

***Corresponding author**

H. Raza

Phone: +97137137506

Fax: +97137672033

E.mail: h.raza@uaeu.ac.ae

Received: 2 July 2009; / Revised: 16 August 2009; / Accepted: 15 December 2009

Abstract

The cytotoxic potential of an antipyretic and analgesic drug, acetaminophen (APAP), was evaluated in mouse J774.2 monocyte macrophages. The cytotoxicity of APAP was evaluated by MTT cell viability and apoptosis assays. Based on the cell viability and apoptosis assays, further experiments were designed with a low (1 $\mu\text{mol/ml}$) and a high (10 $\mu\text{mol/ml}$) dose treatment of APAP in J774.2 cells. Mitochondrial oxidative stress, reactive oxygen species (ROS), mitochondrial glutathione (GSH) metabolism, lipid and protein peroxidation were measured in the drug treated cells. An increase in mitochondrial oxidative stress and ROS production was observed. A decrease in the mitochondrial GSH pool, accompanied by an increase in lipid and protein peroxidation appeared to be the main cause of mitochondrial oxidative stress. GSH pool and GSH metabolizing enzymes were differentially affected in the mitochondria and extramitochondrial compartments. Increased nuclear translocation of NF- κ B-p65, a marker of redox metabolism was also observed in the drug treated cells. In addition, we have demonstrated, for the first time that the mitochondrial aconitase enzyme is a potential ROS-sensitive target in J774.2 cells, which might be used as a marker for APAP-induced cytotoxicity. These results have clearly suggested that APAP induced cytotoxicity in macrophages is mediated by increased mitochondrial oxidative stress and altered redox metabolism. This might have implications in determining the role of circulating macrophages against APAP induced toxicity and cellular defenses in tissues.

Keywords: acetaminophen; apoptosis; glutathione; macrophages J774.2; mitochondria; oxidative stress.

Abbreviation: APAP, N-acetyl para-aminophenol or acetaminophen; COX-2, cyclooxygenase-2; CDNB, Chlorodinitrobenzene; DCFDA, 2',7'-dichloro fluorescein diacetate; DNPH, 2,4-dinitrophenyl hydrazine; GSH, reduced glutathione; GSSG, oxidized glutathione, GST, glutathione S-transferase; GSH-Px, glutathione peroxidase; LPO, lipid peroxidation; MDA, malonaldehyde; MTT, 3-(4,5-dimethylthiazol-2-yl)-2,5-diphenyltetrazolium bromide; NSAIDs, Non-steroidal anti-inflammatory drugs; PMS, post

mitochondrial supernatant; PARP, poly- (ADP)- ribose polymerase; ROS, reactive oxygen species; SDS-PAGE, sodium dodecyl sulfate polyacrylamide gel electrophoresis.

1. Introduction

Overdose of one of the most commonly used analgesic and antipyretic drugs, acetaminophen (APAP) is the leading cause of acute liver poisoning and death globally [1-2]. Physiologically, APAP is primarily activated in the liver, by cytochrome P450s [3-5] to the reactive metabolite N-acetyl-p-benzoquinone imine (NAPQI) which in turn, is efficiently detoxified by conjugation with GSH [6, 7]. However, conjugation at higher doses leads to the critical depletion of GSH which is essential to maintain cellular redox metabolisms causing acute oxidative stress and cellular toxicity. There are numerous studies on the metabolic activation, toxicity and detoxification mechanism of APAP in the liver, kidney and other tissues [5, 8, 9, 10]. Increased mitochondrial stress, production of reactive oxygen and nitrogen species (ROS and RNS respectively) have been implicated in a number of APAP-induced toxicity studies [11-15]. Recent studies have demonstrated that the injured hepatocytes trigger the activation of innate immune cells such as hepatic and circulating macrophages which contribute to the pathophysiology of tissue injury [16-18]. Localized accumulation of macrophages has been observed following toxicant exposure in the tissues. It has also been shown that the modulation of macrophages functioning abrogates the acute toxicity of APAP [19]. The role of macrophages in the pathogenesis of and/or protection from APAP-induced liver toxicity is still controversial. Both, cytoprotective and tissue- destructive roles of macrophages in APAP-induced toxicity have been reported [20-23]. Inactivation of macrophages decreases APAP toxicity presumably by inhibiting the production of ROS and RNS [13]. Supplementation with the antioxidant, glutathione (GSH) as a conjugating agent or the precursor of GSH synthesis, N-acetylcysteine (NAC), which restores intracellular GSH have been proven beneficial in preventing APAP induced cell death both in human and animal models [8,24,25]. However, the precise mechanism of activation,

toxicity and detoxification of this drug in extrahepatic cells, especially in the macrophages, which play a key role in defense against toxicants are not clear. Since the treatment with NAC is not that effective after a certain period (1-2 h) of APAP toxicity in the liver, it is presumed that the restoration of GSH level may not be the only mechanism of preventing APAP-induced toxicity [9, 26, 27]. We, therefore, investigated the effects of APAP on cellular redox metabolism and oxidative stress using a murine monocyte macrophage cell line, J774.2 in culture. Studies have shown that the J774.2 cells exhibited a unique response against the APAP induced effects, which may be associated with the characteristics inhibition of COX-2 enzyme activity [28]. However, there is no further explanation of the mechanism by which APAP induces apoptosis and other adverse effects in these cells. Based on numerous *in vivo* and cell culture studies, we selected a subtoxic lower dose (1 $\mu\text{mol/ml}$) and a higher experimental dose (10 $\mu\text{mol/ml}$) of APAP to elucidate the mechanism by which APAP modulates the cytotoxicity and mitochondrial redox functions in J774.2 cells. We measured the mitochondrial oxidative stress by studying the alterations in the production of reactive oxygen species, lipid and protein peroxidation, and GSH metabolism in the isolated mitochondria from APAP treated cells. In addition, we have also attempted to compare mitochondrial GSH metabolism with extramitochondrial redox metabolism. The expression of an oxidative stress marker, NF- κ B and apoptotic markers cytochrome c and poly-(ADP) - ribose polymerase (PARP) activation was also studied under the above conditions.

2. Materials and methods

2.1 Chemicals

N-Acetyl-p-aminophenol (APAP), glutathione, (GSH and GSSG), 3-(4,5-dimethylthiazol-2-yl)-2,5-diphenyltetrazolium bromide (MTT), NADH, NADPH, 1-chloro-2,4-dinitrobenzene (CDNB), 2,4-dinitrophenylhydrazine (DNPH), lucigenin

and cumene hydroperoxide were purchased from Sigma-Aldrich Fine Chemicals (St Louis, MO, USA). 2', 7'- Dichlorofluorescein diacetate (DCFDA) was from Molecular Probes (Eugene, OR, USA). Apoptosis detection kit for flow cytometry was from BD Pharmingen (BD Biosciences, San Jose, USA). Kits for LPO assay, based on the measurement of total MDA and for aconitase assay were purchased from Oxis International, Inc. (OR, USA). Total NO measurement kits were purchased from R&D Systems, MN, USA. Murine macrophage J774.2 cells were purchased from European Collection of cell cultures (Health Protection Agency Culture Collections, Salisbury, UK). Polyclonal antibodies for NF- κ B, cytochrome c, PARP and beta-actin were purchased from Santa Cruz Biotechnology, Inc, CA, USA. Reagents for cell culture and for SDS-PAGE and Western blot analyses were purchased from Gibco BRL (Grand Island, NY, USA) and from Bio Rad Laboratories (Richmond, CA, USA) respectively.

2.2 Cell culture, treatment and fractionation

Murine macrophage J774.2 cells were grown in poly-L-lysine coated 75 cm² flasks (~2.0-2.5 x10⁶ cells/ml) in DMEM medium supplemented with 10% heat inactivated fetal bovine serum in the presence of 5% CO₂-95% air at 37°C. Cells were treated with different concentrations of APAP (0-10 μ mol/ml or 20 μ mol/ml as in the MTT assay) dissolved in DMSO (final concentration less than 0.2%) and for different time intervals (0.0 to 24 h). Control cells were treated with vehicle alone. Further selection of the doses and time points in this study are based on the published reports as well as on our observation on cytotoxicity assay in J774.2 cells. After the desired time of treatment, cells were harvested, washed with PBS (pH 7.4) and homogenized in H-medium buffer (70 mM sucrose, 220 mM mannitol, 2.5 mM HEPES, 2 mM EDTA, 0.1 and mM phenylmethylsulfonylfluoride, pH7.4) at 4°C. Mitochondria and postmitochondrial (PMS) fractions were prepared by centrifugation and the purity of the isolated fractions for cross contaminations was checked as described before [29, 30].

2.3 MTT cell viability assay

Mitochondrial respiratory function and dehydrogenase based cell viability test in 96 well plates (5 x 10⁴ cells/well) was assayed by MTT conversion to formazan after treatment with different concentrations of APAP for different time intervals essentially as described before [29,30]. The viable cells were quantitated using an ELISA reader (Anthos Laboratories, Salzburg, Germany) at 570 nm after subtracting the appropriate control values.

2.4 Flow cytometry for apoptosis and ROS measurement

The apoptosis assay using flow cytometry was performed as described in the vendor's protocol (BD Pharmingen, BD BioSciences, San Jose, USA). Briefly, cells from 60-70% confluent plates were trypsinized, washed in PBS and resuspended (1x10⁶ cells/ml) in binding buffer (10 mM HEPES, pH 7.4, 140mM NaCl, 2.5mM CaCl₂). A fraction (100 μ l/1x10⁵ cells) of the cell suspension was incubated with 5 μ l Annexin V conjugated to FITC and 5 μ l propidium iodide (PI) for 15 minutes at 25°C in the dark. 400 μ l of binding buffer was added to the suspension and apoptosis was measured immediately using a Becton Dickinson FACScan analyzer. The apoptotic cells were estimated by the percentage of cells that stained positive for Annexin V-FITC while remaining impermeable to PI (AV+/PI-). This method was also able to distinguish viable cells (AV-/PI-) and cells undergoing necrosis (AV-/PI+).

The intracellular production of ROS was measured using the cell permeable probe DCFDA, which preferentially measures peroxides. Briefly, cells (~2 x 10⁶ cells/ml) were incubated with 5 μ M DCFDA for 30 minutes at 37°C. Cells were washed twice with 1X PBS, trypsinized and resuspended in 3 ml of PBS and the fluorescence was immediately read on a Becton Dickinson FACScan with Cell Quest software (BD Biosciences, San Jose, USA). ROS production after APAP treatment was also confirmed by using lucigenin as a probe which is based on the ROS-dependent lucigenin-enhanced chemiluminescence as described before [29,30,32].

ROS sensitive mitochondrial aconitase activity was measured by using the BioxyTech Aconitase-340 assay kit or by using the method as described earlier [31]. Briefly, the assay is based on the indirect measurement of the NADP-dependent conversion of citrate to isocitrate in the presence of isocitrate dehydrogenase. The rate of NADPH formation was then measured in a 1.0 ml assay system consisting of 100 µg mitochondrial protein, 0.2mM NADP, 0.6 mM $MnCl_2$ and 30 mM sodium citrate by following the linear absorbance change at 340 nm after the initial lag.

2.5 Measurement of mitochondrial oxidative stress and redox metabolism

Cells were treated with 1 µmol/ml and 10 µmol/ml APAP for 2 h or 18h and oxidative stress parameters were measured in both the mitochondria and postmitochondrial supernatant (PMS) as described before [29-34]. LPO was measured as the MDA formed using the kit for MDA assay. Protein oxidative damage was measured by DNPH derivatization of oxidized proteins according to the method of Reznick and Packer [35] and Levine et al [36] as described before [37]. Sub cellular GSH levels in the mitochondria and PMS was measured by the NADPH-dependent GSSG-reductase catalyzed conversion of oxidized GSSG to GSH. GST

activity using CDNB, GSH-Px activity using cumene hydroperoxide and GSSG-reductase activity using GSSG-NADPH as the respective substrates were measured by standard protocols as described before [29,30].

2.6 Measurement of the expression of apoptotic markers by SDS-PAGE and Western blot analysis

Proteins (50 µg) from the PMS and nuclear fractions of the cells were separated on 12% SDS-PAGE and electrophoretically transferred on to nitrocellulose paper by Western blotting. The immunoreacting protein bands were visualized after interacting with the antibody against NF-kB, PARP and cytochrome c as described before [29, 30]. The protein bands were quantitated using the gel documentation system (Vilber Lourmat, France) and expressed as relative intensity (R.I) compared to the control bands which are arbitrarily taken as 1.0.

2.7 Statistical analysis

All values shown are expressed as mean \pm SEM of three independent experiments. Statistical significance of the data was assessed by using ANOVA and p values less than (< 0.05) were considered significant.

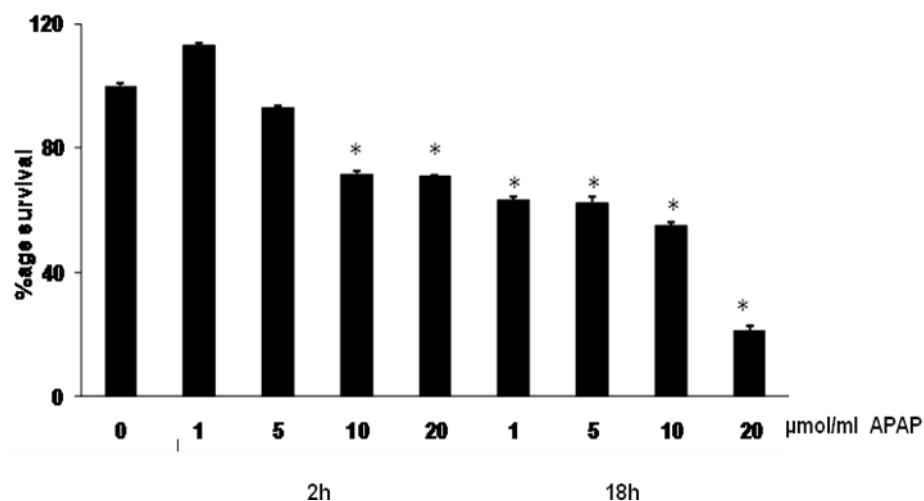


Figure 1: Cell viability assay: Mitochondrial based cell viability assay using MTT reduction was performed after APAP treatment with different doses for 2h and 18h as described in the Materials and Methods. The values are mean \pm SEM for three determinations. Asterisks indicate significant difference ($p < 0.05$) from control values.

3. Results

3.1 Effect of APAP on cell viability

A gradual decrease in cell survival with increasing concentrations of APAP was observed (Figure 1). At the lower pharmacological dose (1-5 $\mu\text{mol/ml}$) of APAP, no significant alteration in cell viability (5-10% inhibition) was observed in 2 h. The maximum inhibition (~80%) was, however, observed in cells treated with 20 $\mu\text{mol/ml}$ APAP for 18 h.

3.2 Effect of APAP on apoptosis and mitochondrial oxidative stress

As shown in Figure 2, the apoptosis assay by flow cytometry has demonstrated that increasing doses and durations of APAP treatment caused increased apoptosis (shown as % in upper right quadrant) in the macrophage cells. While 2 h of APAP treatment showed no significant increase in apoptosis, the 1 $\mu\text{mol/ml}$ and 10 $\mu\text{mol/ml}$ APAP caused about 25% and 50% increase in apoptosis after 18 h respectively.

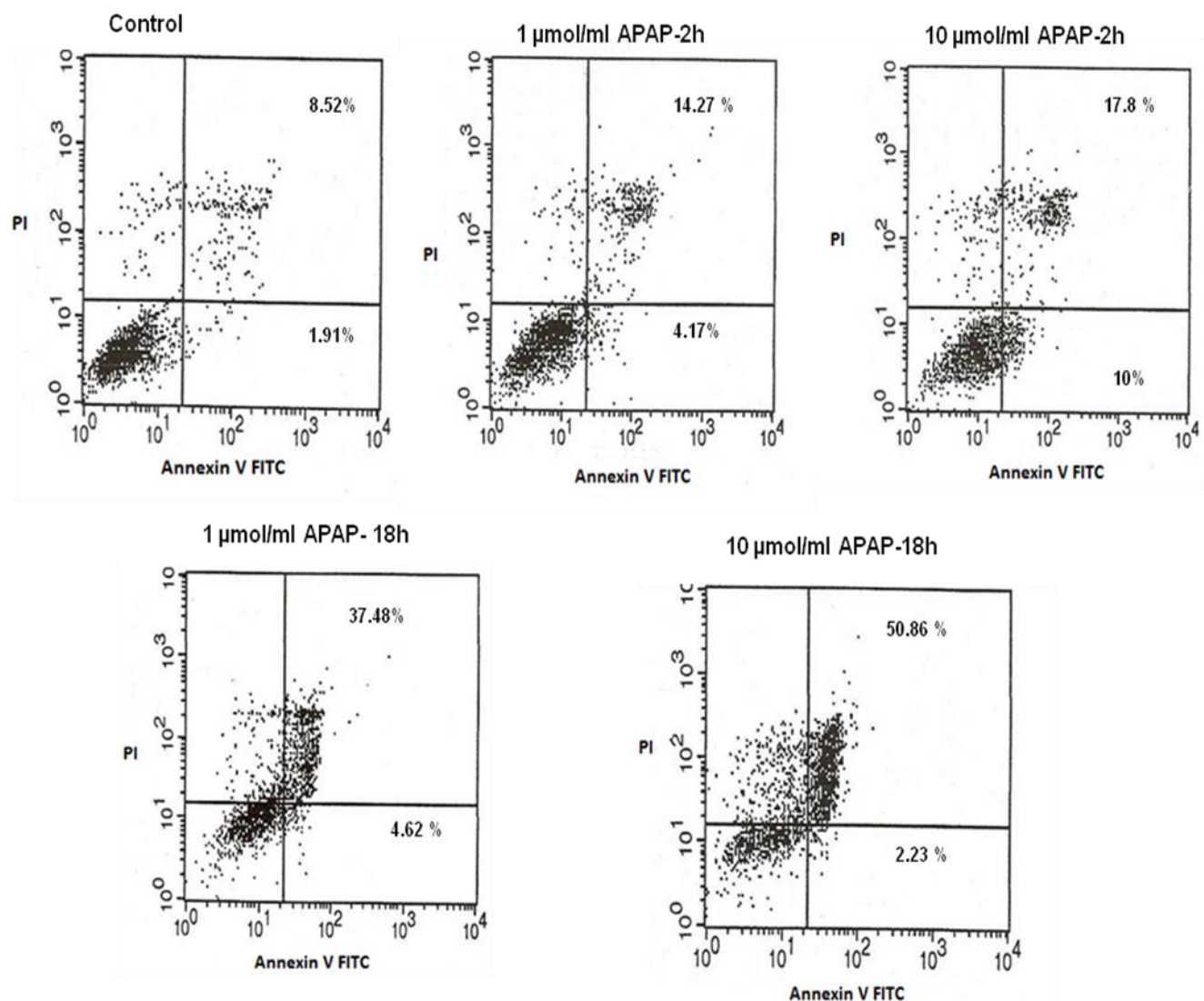


Figure 2: Apoptosis assay by flow cytometry: Apoptosis in J774.2 cells was measured after APAP treatment using Flow cytometry as described in the Materials and Methods using the Becton Dickinson FACScan analyser. Apoptotic cells were estimated by the percentage of cells that stained positive for Annexin V-FITC. The percentage apoptosis is shown in the upper right quadrant. The figure shown is representative analysis from atleast three experiments.

Using DCFDA as a fluorescent probe, we observed a significant dose- and time-dependent increase (30-40%) in ROS production after APAP treatment (Figure 3A). As shown, both 1 $\mu\text{mol/ml}$ and 10 $\mu\text{mol/ml}$ APAP caused increased ROS production only after 18 h of treatment. This was further confirmed by using an additional lucigenin chemiluminescent assay (Figure 3B)

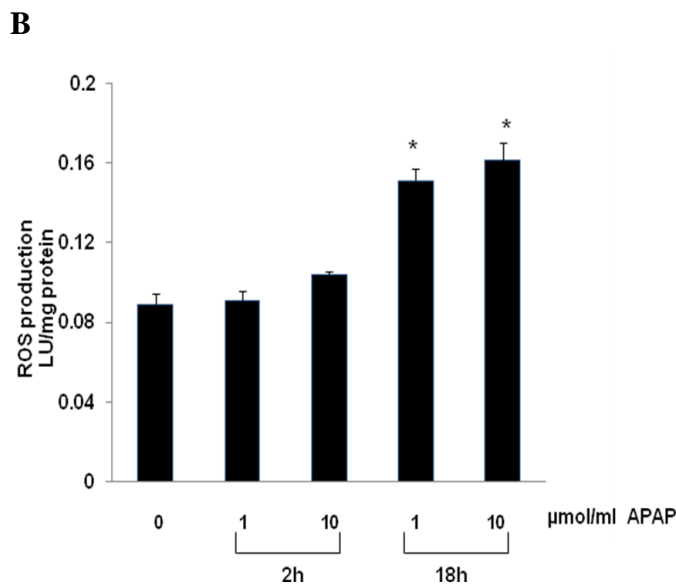
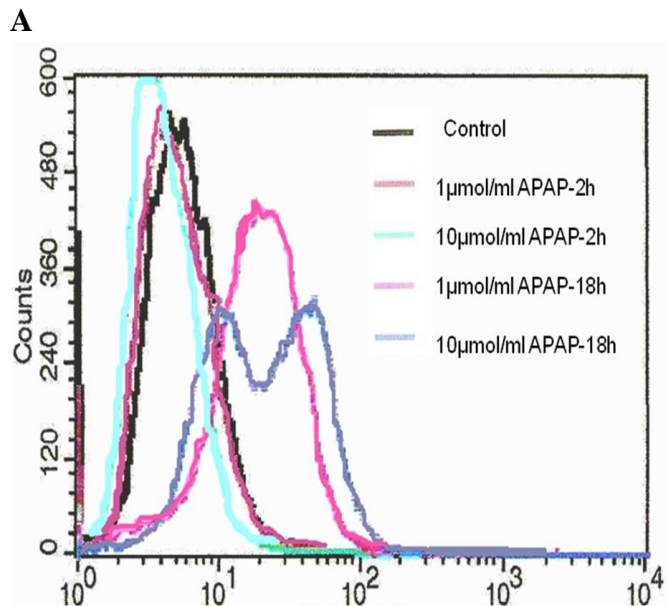


Figure 3A, B: ROS assay: The intracellular production of ROS was measured in J774.2 cells treated with APAP using DCFDA and fluorescence was measured by flow cytometry (A) using Cell Quest software as

described in the Materials and Methods. Result expressed is a typical representation of at least three individual experiments. ROS production was further confirmed by luminometry using lucigenin as a probe (B) as described in the Materials and Methods. The values are mean \pm SEM for at least three independent assays. Asterisks indicate significant difference ($p > 0.05$) from control values.

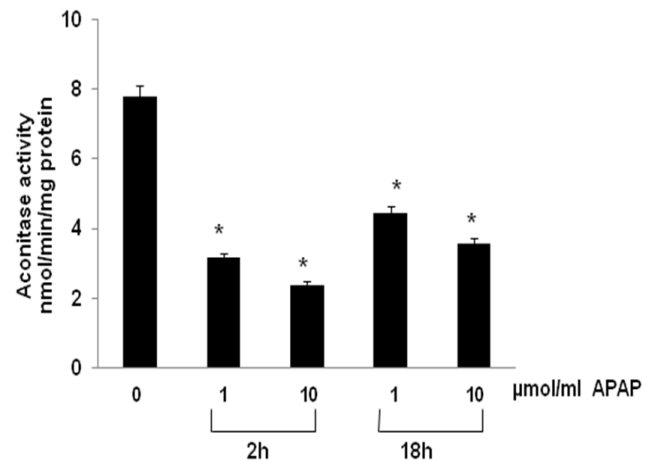


Figure 3C: Mitochondrial aconitase assay: Freshly isolated mitochondria (100 μg protein) was used to assay aconitase activity using an isocitrate coupling system by NADPH formation as described in the Materials and Methods. The values are mean \pm SEM for at least three independent assays. Asterisks indicate significant difference ($p > 0.05$) from control values.

The aconitase activity is highly sensitive to mitochondrial ROS production. For the first time, we have shown a marked inhibition in ROS sensitive aconitase activity in J774.2 cells after APAP treatment (Figure 3C) confirming the increased mitochondrial oxidative stress. The higher dose (10 $\mu\text{mol/ml}$) of APAP seemed to be more inhibitory than the lower dose (1 $\mu\text{mol/ml}$). The activity, however, appeared to be affected more after two hours of APAP treatment (upto 72% inhibition) compared to the treatment after 18 h (52% inhibition).

Mitochondrial oxidative stress was further analyzed by studying membrane LPO and protein carbonylation. 10 $\mu\text{mol/ml}$ APAP treatment for 18 h caused a 4 fold increase in membrane LPO in the mitochondria (Figure 4A) and about 2 fold

increase in the extramitochondrial PMS fraction (Figure 4B). Protein peroxidation, as measured by DNPH derivatization of oxidized proteins, was markedly increased (3-4 fold) after APAP treatment for 18 h (Figure 5). A 2-fold increase in protein carbonylation was also observed with 10 $\mu\text{mol/ml}$ APAP treatment for 2 h. All these data strongly suggest the increased oxidative stress in APAP treated macrophages.

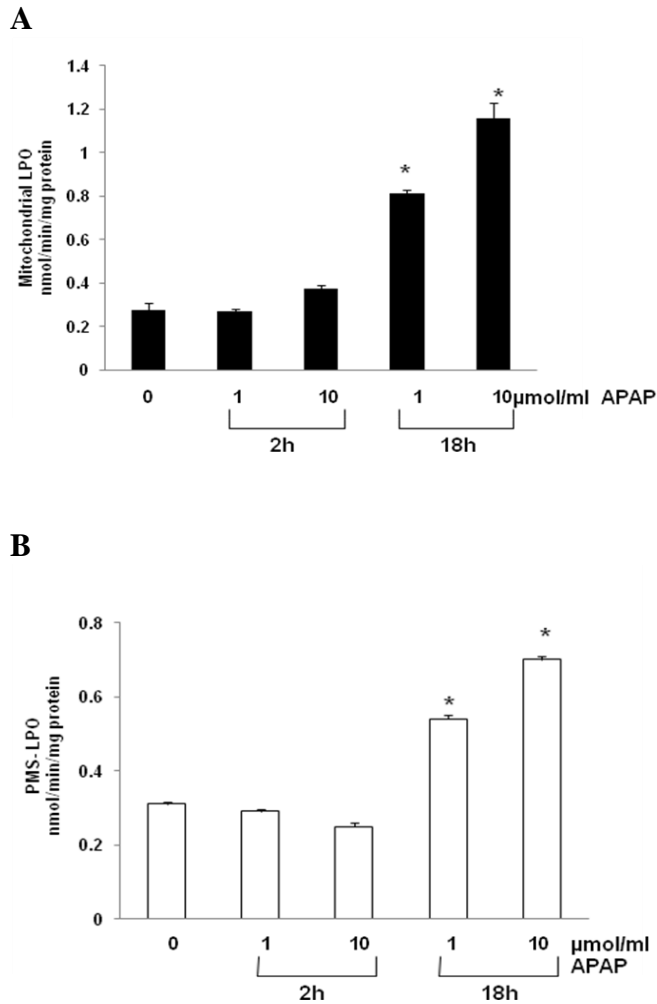


Figure 4 A, B: LPO assay: Lipid peroxidation was measured in the mitochondria (A) and PMS (B) as total MDA formation using a kit from Oxis International as described in the Materials and Methods. The values are mean \pm SEM for three individual assays. Asterisks indicate significant difference ($p < 0.05$) from control values.

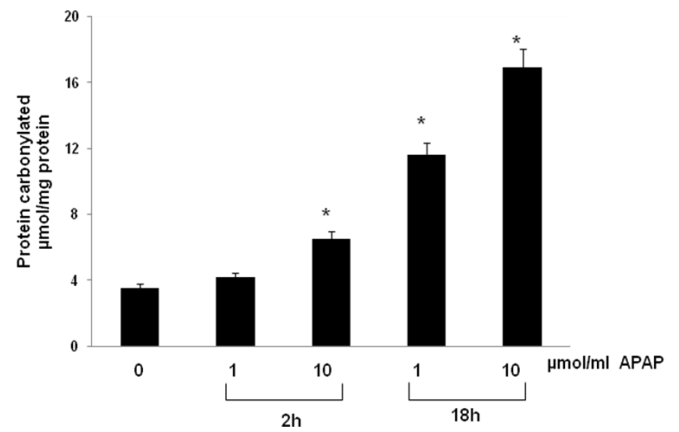


Figure 5: Protein oxidative carbonylation assay was based on the coupling of APAP treated cellular fractions with DNPH and measuring the derivatized protein spectrophotometrically at 270 nm. The values are mean \pm SEM for three determinations. Asterisks indicate significant difference ($p < 0.05$) from control values.

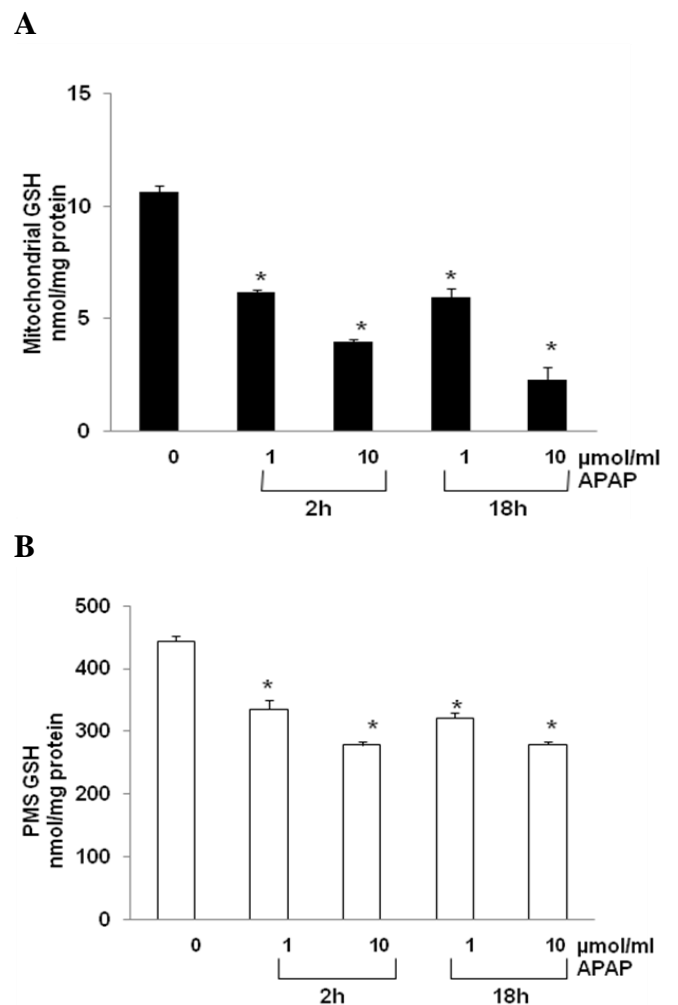


Figure 6A, B: GSH assay J774.2 cells were treated with APAP and GSH levels in the mitochondria (A)

and PMS (B) were measured by enzymatic method as described in the Materials and Methods. Results are expressed as mean \pm SEM of three independent assays. Asterisks indicate significant difference ($p < 0.05$) from untreated cells.

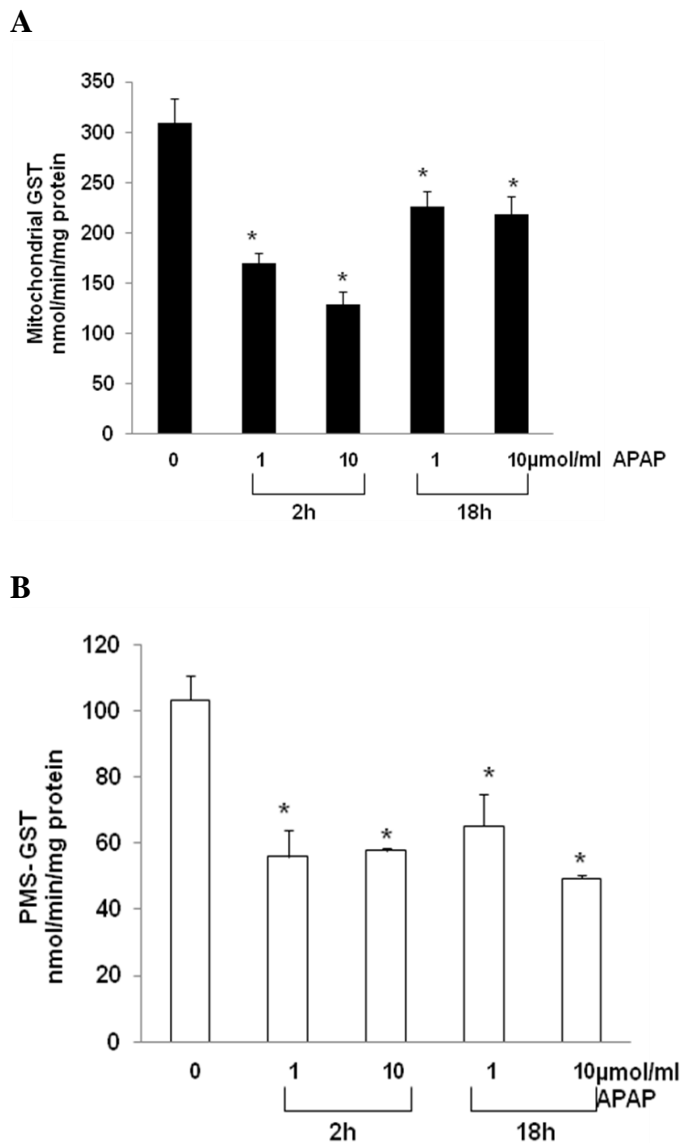


Figure 7A, B: GST-CDNB assay: Mitochondrial and PMS fractions were isolated from APAP treated J744.2 cells for the assay of GSH metabolizing enzymes using standard substrates as described [29, 30] in the Materials and Methods in the mitochondria (A) and PMS (B). Glutathione S-transferase assay was performed with CDNB as described in the Materials and Methods. Results are expressed as mean \pm SEM of three independent assays. Asterisks indicate significant difference ($p < 0.05$) from untreated cells.

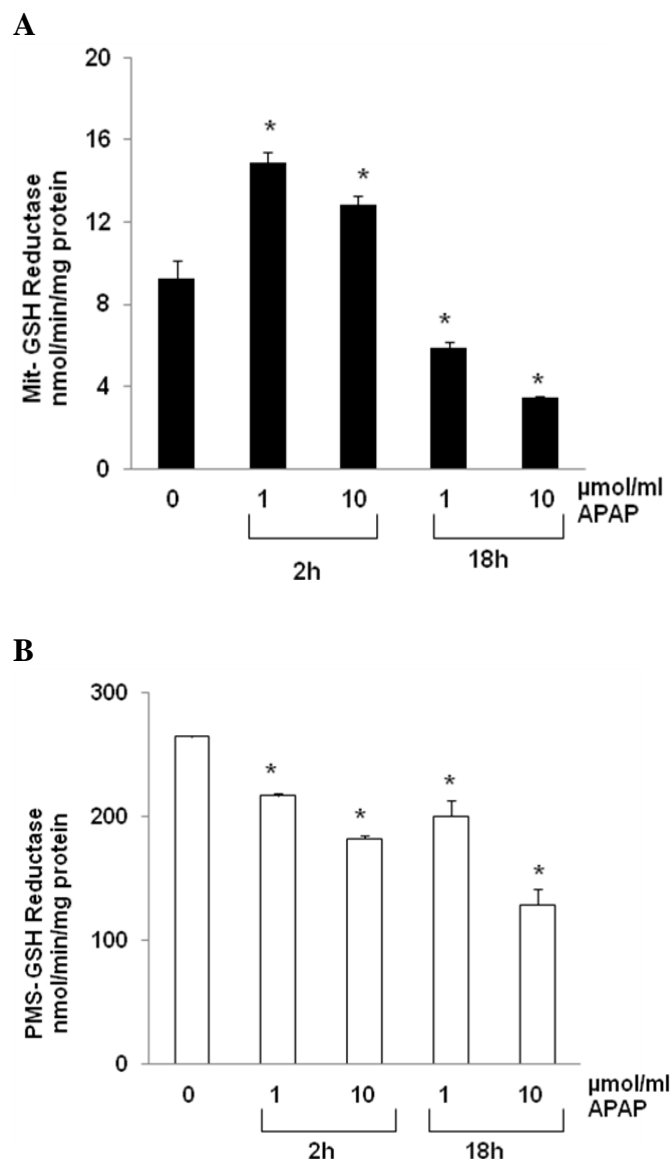


Figure 8A, B: GSSG-reductase assay was performed with GSSG/NADP as the substrate in the mitochondria (A) and PMS (B) as described in the Materials and Methods. Results are expressed as mean \pm SEM of three independent assays. Asterisks indicate significant difference ($p < 0.05$) from untreated cells.

3.3 Effect of APAP on mitochondrial GSH metabolism

The total GSH pool was significantly decreased, both in the mitochondria (2-3 fold) (Figure 6A) and the PMS (~ 40-50%) (Figure 6B). Activity of the GSH metabolizing enzyme, GST was inhibited significantly (50-60%) initially, both in the mitochondria and PMS (Figure 7A and B).

A low recovery was, however, observed after 18 h of drug exposure which was still significantly A

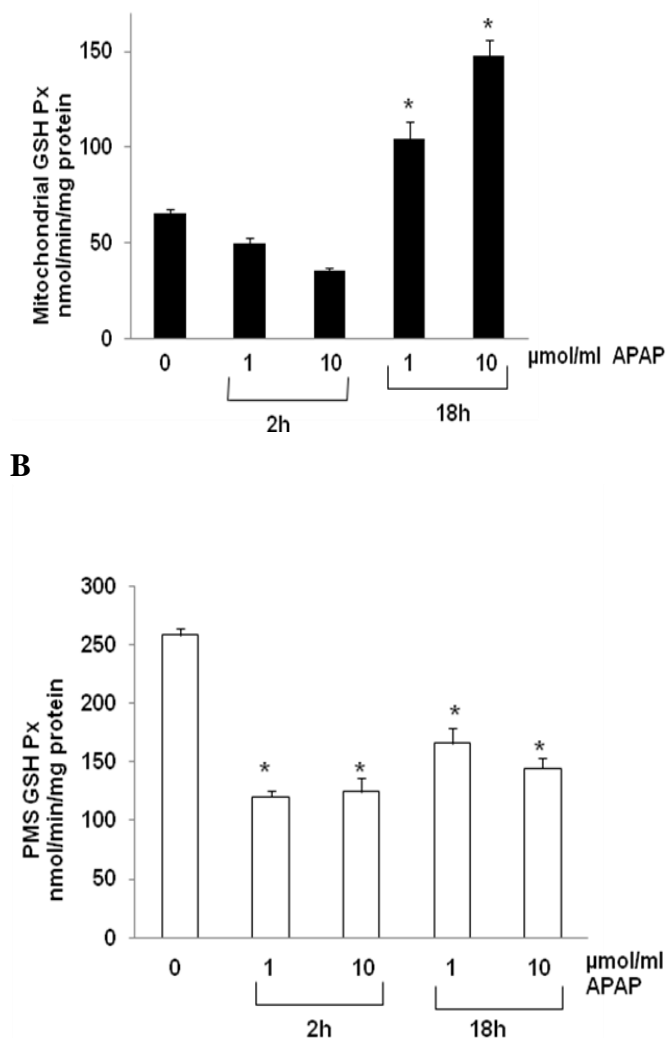


Figure 9A, B: GSH-peroxidase assay was performed with cumene hydroperoxide as a substrate in the mitochondria (A) and PMS (B) as described in the Materials and Methods. The values are mean \pm SEM for three independent assays. Asterisks indicate significant difference ($p < 0.05$) from control values.

lower than control values. This may suggest alterations in the rate of APAP metabolism and conjugation with GSH. Mitochondrial GSH reductase activity showed a significant increase initially in 2 h, followed by a marked decrease in activity with 10 $\mu\text{mol/ml}$ APAP in 18 h (Figure

8A). PMS showed a significant decrease (30-50%) in reductase activity with increasing dose of APAP (Figure 8B). In contrast, a decrease (50%) in the mitochondrial GSH-Px activity was observed within 2 h of treatment which was followed by a marked increase after 18h (Figure 9A). In the PMS, however, the activity remained decreased even after 18 h of treatment. These discrepancies may reflect different rates of regeneration of GSH pools in the mitochondria and extramitochondrial compartments.

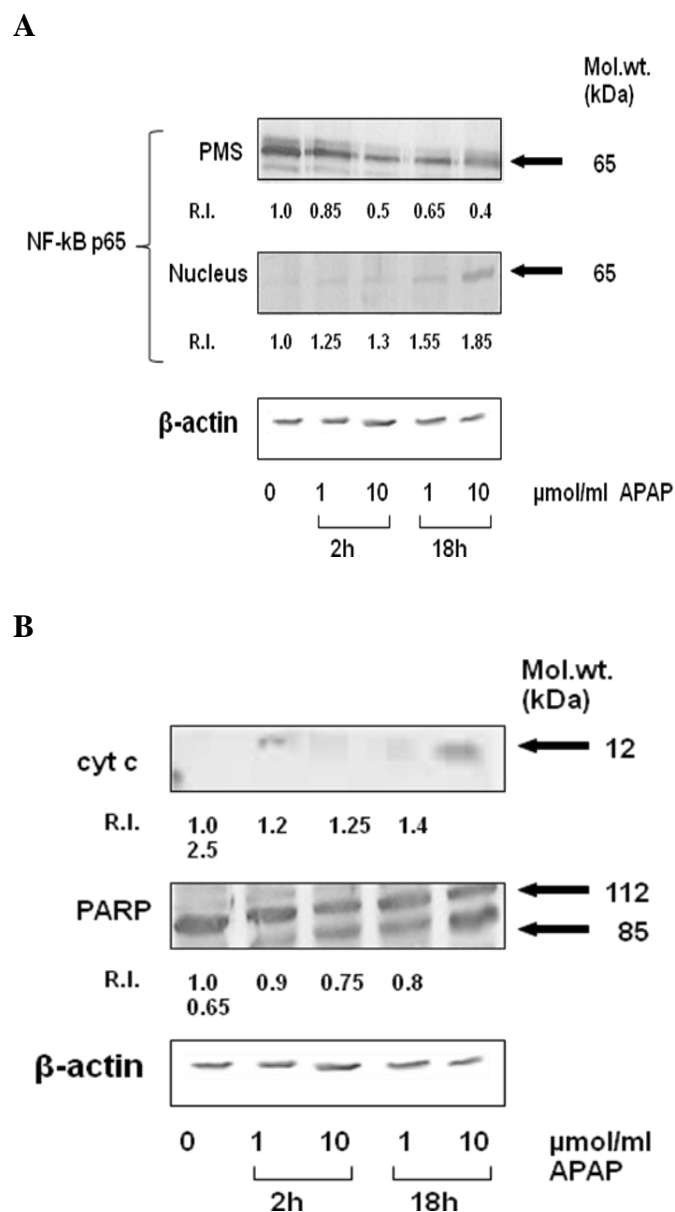


Figure 10A, B: Expression of apoptotic markers: Proteins (50 μg) from the nuclear and PMS fractions

were separated on the 12% SDS-PAGE and Western blotting was performed as before [29, 30]. The expression of NF- κ B (A), cytochrome c and PARP (B) was measured by probing with the antibody against the specific protein. Quantitation of visualized protein bands was done by densitometry and the results were expressed as relative intensity (R.I.) using control untreated values as 1.0. Beta-actin was used as a loading control.

3.4 Effect of APAP on the expression of apoptotic markers

Figure 10A shows the increased translocation of NF- κ B into the nucleus of APAP treated cells. This effect was more apparent with 10 μ mol/ml treatment after 18 h compared to the 1 μ mol/ml treatment. In support to our observation of increased apoptosis, the SDS-PAGE analysis has demonstrated an increased release of cytochrome c from the mitochondria which was accompanied by an increased (apoptosis) processing of the DNA repair enzyme PARP (Figure 10B).

4. Discussion

The NSAIDs have antipyretic, analgesic and anti-inflammatory properties albeit with differential effects upon treatment. This may be due to the differences in their half-lives, metabolism and effects on arachidonic acid metabolism and COX inhibition [38]. APAP has antipyretic and analgesic effects, as are NSAIDs, but has minimum effect as an anti-inflammatory drug. In response to various stimuli, COX-2 is highly inducible in macrophages [39]. Presumably, there are COX variants which respond differently with NSAIDs or other drugs like, APAP [28]. Most of the studies on APAP are focused on the toxicity in the liver or liver cells. However, the molecular mechanism(s) by which APAP exert their pharmacological or cytotoxic effects in circulating macrophages, is still not clear. This is partly due to the existence of subpopulations of tissue specific resident (like Kupffer cells) and circulating macrophages [23]. APAP induces cytotoxicity and apoptosis in a variety of tissues and cellular populations through mitochondrial dependent pathways [6, 7, 15]. Our present study, using J774.2 macrophages, also shows that APAP-induced cytotoxicity and

apoptosis is associated with increased mitochondrial oxidative stress, ROS production, and alterations in the GSH pool. Impaired GSH metabolism and antioxidant defenses by APAP have implications in the pathogenesis of a number of inflammatory diseases where macrophages play significant cytoprotective roles [7, 23, 40, 41]. GSH and GSH-Px are mainly responsible in detoxifying the ROS and RNS in APAP-induced cytotoxicity [25]. Our results demonstrate that the GSH pool is markedly diminished in APAP-treated J774.2 cells, especially in the mitochondria and this effect is coupled with the significant decrease in GSH conjugating enzyme, glutathione S-transferase. GSH-peroxidase activity was initially inhibited by APAP treatment in the mitochondria which increased after 18 h of drug treatment. Initial increase in GSSG-reductase activity in the mitochondria by APAP suggests the activation of the defense mechanism by recycling the oxidized GSSG to reduced GSH to protect the cells against the ROS mediated damages. However, GSSG reductase activity was inhibited after 18 h, which supports the observation of a decreased GSH pool after drug treatment. [7, 11, 42]. A significant increase in LPO was observed after 18 h of APAP treatment. On the other hand, after 2 h of drug treatment a significant increase in mitochondrial LPO was observed with 10 μ mol/ml APAP treatment while in the PMS no significant alterations were observed either with 1 μ mol/ml or 10 μ mol/ml APAP. Our data also demonstrates that APAP increases nuclear translocation of the transcription factor, NF- κ B, in J774.2 cells, which is activated in inflammatory responses as seen during increased oxidative stress conditions [43, 44]. We have further confirmed increased mitochondrial oxidative stress in APAP-treated J774.2 cells by a marked inhibition of ROS sensitive aconitase enzyme. Our results also demonstrate that 2 h treatment of APAP was more effective than 18 h treatment. This may be associated with the metabolism of APAP suggesting the parent compound to be more potent in inhibiting the aconitase activity. In our recent publications, using various in vivo and in vitro cell culture models, it has been shown that mitochondrial respiratory and redox metabolisms

are specifically affected under increased oxidative stress conditions [29-34, 45]

5. Conclusion

In summary, using a circulating monocyte macrophage J774.2 cell line, we have demonstrated that acetaminophen induces apoptosis and oxidative stress primarily by increasing the ROS production and altering GSH metabolism. The GSH pool was differently and markedly affected in the mitochondria compared to the extramitochondrial compartment. Increased activation of inflammatory and oxidative stress responsive transcription factor NF- κ B also observed in these cells treated with APAP. A similar study is being planned using freshly isolated monocytes from humans. Our study, for the first time, demonstrates that the mitochondrial enzyme, aconitase is a sensitive marker for APAP-induced cytotoxicity.

Acknowledgements

This study is partly supported by a Research Grant from the FMHS Research Committee and from the Terry Fox Cancer Research Fund. A support from the FMHS Graduate Committee Funds (for TAB) is also acknowledged. Authors wish to thank Dr Maria Cabezudo, Department of Biochemistry, for her help in the flow cytometry assays.

References

1. Litovitz, T.L.; Klein-Schwartz, W.; Rodgers, G.C. Jr.; Coughlin, D.J.; Youniss, J.; Omslaer, J.C.; May, M.E.; Woolf, A.D.; Benson, B.E. 2001 Annual report of the American Association of Poison Control Centers Toxic Exposure Surveillance System, *Am J Emerg Med*, 2002, 20,391-452.
2. Lazerow, S.K.; Abdi, M.S.; Lewis, J.H. Drug-induced liver disease 2004, *Curr Opin Gastroenterol*, 2005, 21, 283-292.
3. Chen, W.; Koenigs, L.L.; Thompson, S.J.; Peter, R.M.; Rettie, A.E.; Trager, W.F.; Nelson, S.D. Oxidation of acetaminophen to its toxic quinone imine and nontoxic catechol metabolites by baculovirus-expressed and purified human cytochromes P450 2E1 and 2A6, *Chem Res Toxicol*, 1998,11,295-301.
4. Patten, C.J.; Thomas, P.E.; Guy, R.L.; Lee, M.; Gonzalez, F.J.; Guengerich, F.P.; Yang, C.S. Cytochrome P450 enzymes involved in acetaminophen activation by rat and human liver microsomes and their kinetics, *Chem Res Toxicol*, 1993, 6,511-518.
5. Nelson, S.D. Molecular mechanism of the hepatotoxicity caused by acetaminophen, *Semin liver Dis*, 10, 267-278.
6. Hinson, J.A.; Reid, A.B.; McCullough, S.S.; James, L.P. Acetaminophen-induced hepatotoxicity: role of metabolic activation, reactive oxygen/nitrogen species, and mitochondrial permeability transition, *Drug Metab Rev*, 2004, 36, 805-822.
7. Reid, A.B.; Kurten, R.C.; McCullough, S.S.; Brock, R.W.; Hinson, J.A. Mechanisms of acetaminophen-induced hepatotoxicity: role of oxidative stress and mitochondrial permeability transition in freshly isolated mouse hepatocytes, *J Pharmacol Exp Ther*, 2005, 312, 509-516.
8. Bajt, M.L.; Knight, T.R.; Lemasters, J.J.; Jaeschke, H. Acetaminophen-induced oxidant stress and cell injury in cultured mouse hepatocytes: protection by N-acetyl cysteine, *Toxicol Sci*, 2004, 80, 343-349.
9. Botta, D.; Shi, S.; White, C.C.; Dabrowski, M.J.; Keener, C.L.; Srinouanprachanh, S.L.; Farin, F.M.; Ware, C.B.; Ladiges, W.C.; Pierce, R.H.; Fausto, N.; Kavanagh, T.J. Acetaminophen-induced liver injury is attenuated in male glutamate-cysteine ligase transgenic mice, *J. Biol Chem*, 2006, 281, 28865-28875.
10. Bessems, J.G.; Vermeulen, N.P. Paracetamol (acetaminophen)-induced toxicity: molecular and biochemical mechanisms, analogues and protective approaches, *Crit Rev Toxicol*, 2001, 31, 55-138.
11. James, L.P.; Mayeux, P.R.; Hinson, J.A. Acetaminophen-induced hepatotoxicity, *Drug Metab Dispos*, 2003, 31, 1499-1506.
12. Boobis, A.R.; Tee, L.B.; Hampden, C.E.; Davies, D.S. Freshly isolated hepatocytes as a

- model for studying the toxicity of paracetamol, *Food Chem Toxicol*, 1986, 24, 731-736.
13. Michael, S.L.; Pumford, N.R.; Mayeux, P.R.; Niesman, M.R.; Hinson, J.A. Pretreatment of mice with macrophage inactivators decreases acetaminophen hepatotoxicity and the formation of reactive oxygen and nitrogen species, *Hepatology*, 1999, 30, 186-195.
 14. Jaeschke, H.; Knight, T.R.; Bajt, M.L. The role of oxidant stress and reactive nitrogen species in acetaminophen hepatotoxicity, *Toxicol Lett*, 2003, 144, 279-288.
 15. Andringa, K.K.; Bajt, M.L.; Jaeschke, H.; Bailey, S.M. Mitochondrial protein thiol modifications in acetaminophen hepatotoxicity: effect on HMG-CoA synthase, *Toxicol Lett*, 2008, 177, 188-197.
 16. Ito, Y.; Abril, E.R.; Bethea, N.W.; McCuskey, R.S. Ethanol binging enhances hepatic microvascular responses to acetaminophen in mice, *Microcirculation*, 2004, 11, 625-632.
 17. Liu, Z.X.; Govindarajan, S.; Kaplowitz, N. Innate immune system plays a critical role in determining the progression and severity of acetaminophen hepatotoxicity, *Gastroenterology*, 2004, 127, 1760-1774.
 18. Liu, Z.X.; Han, D.; Gunawan, B.; Kaplowitz, N. Neutrophil depletion protects against murine acetaminophen hepatotoxicity, *Hepatology*, 2006, 43, 1220-1230.
 19. Laskin, D.L.; Gardner, C.R.; Price, V.F.; Jollow, D.J. Modulation of macrophage functioning abrogates the acute hepatotoxicity of acetaminophen, *Hepatology*, 1995, 21, 1045-1050.
 20. Ju, C.; Reilly, T.P.; Bourdi, M.; Radonovich, M.F.; Brady, J.N.; George, J.W.; Pohl, L.R. Protective role of Kupffer cells in acetaminophen-induced hepatic injury in mice, *Chem Res Toxicol*, 2002, 15, 1504-1513.
 21. Gordon, S. Alternative activation of macrophages, *Nat Rev Immunol*, 2003, 3, 23-35.
 22. Ishida, Y.; Kondo, T.; Kimura, A.; Tsuneyama, K.; Takayasu, T.; Mukaida, N. Opposite roles of neutrophils and macrophages in the pathogenesis of acetaminophen-induced acute liver injury, *Eur J Immunol*, 2006, 36, 1028-1038.
 23. Holt, M.P.; Cheng, L.; Ju, C. Identification and characterization of infiltrating macrophages in acetaminophen-induced liver injury, *J Leukoc Biol*, 2008, 84, 1410-1421.
 24. Jaeschke, H.; Gujral, J.S.; Bajt, M.L. Apoptosis and necrosis in liver disease, *Liver Int*, 2004, 24, 85-109. Review.
 25. Knight, T.R.; Ho, Y.S.; Farhood, A.; Jaeschke, H. Proxynitrite is a critical mediator of acetaminophen hepatotoxicity in murine livers: protection by glutathione, *J Pharmacol Exp Ther*, 2002, 303, 468-475.
 26. Beyer, R.P.; Fry, R.C.; Lasarev, M.R.; McConnachie, L.A.; Meira, L.B.; Palmer, V.S.; Powell, C.L.; Ross, P.K.; Bammler, T.K.; Bradford, B.U.; Cranson, A.B.; Cunningham, M.L.; Fannin, R.D.; Higgins, G.M.; Hurban, P.; Kayton, R.J.; Kerr, K.F.; Kosyk, O.; Lobenhofer, E.K.; Sieber, S.O.; Vliet, P.A.; Weis, B.K.; Wolfinger, R.; Woods, C.G.; Freedman, J.H.; Linney, E.; Kaufmann, W.K.; Kavanagh, T.J.; Paules, R.S.; Rusyn, I.; Samson, L.D.; Spencer, P.S.; Suk, W.; Tennant, R.J.; Zarbl, H.; Members of the Toxicogenomics Research Consortium. Multicenter study of acetaminophen hepatotoxicity reveals the importance of biological endpoints in genomic analyses, *Toxicol Sci*, 2007, 99, 326-337.
 27. Manov, I.; Hirsh, M.; Iancu, T. C. N-acetylcysteine does not protect HepG2 cells against acetaminophen-induced apoptosis, *Basic Clin Pharmacol Toxicol*, 2004, 94, 213-225.
 28. Simmons, D.L.; Wagner, D.; Westover, K. Nonsteroidal anti-inflammatory drugs, acetaminophen, cyclooxygenase 2, and fever, *Clin Infect Dis*, 2000, 31, S211-S218.
 29. Raza, H.; John, A. Green tea polyphenol epigallocatechin-3-gallate differentially modulates oxidative stress in PC12 cell compartments, *Toxicol App Pharmacol*, 2005, 207, 212-220.
 30. Raza, H.; John, A. 4-Hydroxynonenal induces mitochondrial oxidative stress, apoptosis and expression of glutathione S-transferase A4-4 and cytochrome P450 2E1 in PC12 cells, *Toxicol App Pharmacol*, 2006, 216, 309-318.

31. Spear, J.F.; Prabu, S.K.; Galati, D.; Raza, H.; Anandatheerthavarada, H.K.; Avadhani, N.G. Beta 1 Adrenoreceptor activation contributes to ischemia/reperfusion damage as well as plays a role in ischemic preconditioning, *Am J Physiol Heart and Circ Physiol*, 2007, 292, H2459-H2466.
32. Raza, H.; Prabu, S.K.; Robin, M.A.; Avadhani, N.G. Elevated mitochondrial cytochrome P450 2E1 and glutathione S-transferase A4-4 in streptozotocin-induced diabetic rats: tissue-specific variations and roles in oxidative stress, *Diabetes*, 2004, 53, 185-194.
33. Raza, H.; Robin, M.A.; Fang, J.K.; Avadhani, N.G. Multiple isoforms of mitochondrial glutathione S-transferases and their differential induction under oxidative stress, *Biochem J*, 2002, 366, 45-55.
34. Prabu, S.K.; Anandatheerthavarada, H.K.; Raza, H.; Srinivasan, S.; Spear, J.F.; Avadhani, N.G. Protein kinase A-mediated phosphorylation modulates cytochrome C oxidase function and augments hypoxia and myocardial ischemia related injury, *J Biol Chem*, 2006, 281, 2061-2070.
35. Reznick, A.Z.; Packer, L. Oxidative damage to proteins: spectrophotometric method for carbonyl assay, *Methods Enzymol*, 1994, 233, 357-363.
36. Levine, R.L.; Williams, J.A.; Stadtman, E.R.; Shacter, E. Carbonyl assays for determination of oxidatively modified proteins, *Methods Enzymol*, 1994, 233, 346-357.
37. Raza, H.; John, A. In vitro protection of reactive oxygen species-induced degradation of lipids, proteins and 2-deoxyribose by tea catechins, *Food Chem Toxicol*, 2007, 45, 1814-1820.
38. Insel, P.A. Analgesic-antipyretics and anti-inflammatory agents: drugs employed in the treatment of rheumatoid arthritis and gout. In: *The pharmacological basis of therapeutics*, Gliman, A.G.; Rall, T.W.; Nies, A.S.; Taylor, P.; Elmsford, N.Y.; Ed.; Pergamon Press, Inc, 1990; pp636-681.
39. Kujubu, D.A.; Fletcher, B.S.; Varnum, B.C.; Lim, R.W.; Herschman, H.R. TIS10, a phorbol ester tumor-promoter-inducible mRNA from Swiss 3T3 cells, encodes a novel prostaglandin synthase/cyclooxygenase homologue, *J Biol Chem*, 1991, 266, 12866-12872.
40. Dimova, S.; Hoet, P.H.; Dinsdale, D.; Nemery, B. Acetaminophen decreases intracellular glutathione levels and modulates cytokine production in human alveolar macrophages and type II pneumocytes in vitro, *Int J Biochem Cell Biol*, 2005, 37, 1727-1737.
41. Ryu, Y.S.; Lee, J.H.; Seok, J.H.; Hong, J.H.; Lee, Y.S.; Lim, J.H.; Kim, Y.M.; Hur, G.M. Acetaminophen inhibits iNOS gene expression in RAW 264.7 macrophages: differential regulation of NF-kappaB by acetaminophen and salicylates, *Biochem Biophys Res Commun*, 2000, 272, 758-764.
42. Knight, T.R.; Fariss, M.W.; Farhood, A.; Jaeschke, H. Role of lipid peroxidation as a mechanism of liver injury after acetaminophen overdose in mice, *Toxicol Sci*, 2003, 76, 229-236.
43. Gardner, C.R.; Laskin, J.D.; Dambach, D.M.; Chiu, H.; Durham, S.K.; Zhou, P.; Bruno, M.; Gerecke, D.R.; Gordon, M.K.; Laskin, D.L. Exaggerated hepatotoxicity of acetaminophen in mice lacking tumor necrosis factor receptor-1. Potential role of inflammatory mediators, *Toxicol Appl Pharmacol*, 2003, 192, 119-130.
44. Dambach, D.M.; Durham, S.K.; Laskin, J.D.; Laskin, D.L. Distinct roles of NF-kappaB p50 in the regulation of acetaminophen-induced inflammatory mediator production and hepatotoxicity, *Toxicol Appl Pharmacol*, 2006, 211, 157-165.
45. Raza, H.; John, A.; Brown, E.M.; Benedict, S.; Kambal, A. Alterations in mitochondrial respiratory functions, redox metabolism and apoptosis by oxidant 4-hydroxynonenal and antioxidants curcumin and melatonin in PC12 cells, *Toxicol Appl Pharmacol*, 2008, 226, 161-168.